Distinct Western North Pacific Tropical Cyclogenesis During Inactive Intraseasonal Phase of August 1996 and 2014

Xi Cao (caoxi09@mail.iap.ac.cn)
Institute of Atmospheric Physics Chinese Academy of Sciences https://orcid.org/0000-0002-2064-7018

Renguang Wu
Zhejiang University

Jing Xu
China Academy of Meteorological Sciences

Yifeng Dai
Tongji Zhejiang College

Mingyu Bi
Nanjing University of Information Science and Technology

Xiaoqing Lan
Chinese Academy of Sciences

Xiping Zhang
CMA STI: China Meteorological Administration Shanghai Typhoon Institute

Research Article

Keywords: TC genesis, environmental factors, the western North Pacific, inactive intraseasonal phase.

Posted Date: May 18th, 2021

DOI: https://doi.org/10.21203/rs.3.rs-516694/v1

Abstract

While intraseasonal oscillation was in the inactive phase over the western North Pacific (WNP) during August of 1996 and 2014, no tropical cyclone (TC) genesis occurred in August of 2014, whereas 9 TCs (average 5.7 TCs) formed in August of 1996 with 5 TCs in the northeastern part (the largest number since 1979) and 4 TCs in the southwestern part. The present analysis reveals an obvious southwest-northeast-oriented lower-level wave train over the WNP associated with anomalous convection around the Maritime Continent in August 1996. This wave train induced anomalous cyclone and enhanced convection over the northeastern WNP, which provided a favorable background for TC genesis. Over the southwestern WNP, although monthly mean anomalies were unfavorable, the intraseasonal variation contributed to positive vorticity anomalies at the time and location of TC genesis. In contrast, both monthly anomalies and daily variations of environment factors were hostile to TC genesis during August 2014.

1. Introduction

The western North Pacific (WNP) is the basin of the most active tropical cyclone (TC) genesis on earth with an average of 26 cases each year, accounting for about one-third of global annual TCs. The lower-level winds in the TC peak seasons over the WNP feature a zonal convergence and a meridional shear line between the westerlies and the easterlies, which provide a favorable background for the TC genesis (Ritchie and Holland, 1999; Li, 2012; Wu et al., 2012; Molinari and Vollaro, 2013). The TC genesis over the WNP is strongly influenced by the Madden–Julian oscillation (MJO), a primary signal of intraseasonal oscillation (ISO) (e.g., Liebmann et al., 1994; Madden and Julian, 1994; Maloney and Hartmann, 2001; Camargo et al., 2009; Huang et al., 2011; Zhao and Li, 2019; Cao and Wu, 2020). It is commonly accepted that more TCs tend to form during the active MJO phase and less TCs tend to form during the inactive MJO phase over the WNP. The MJO modulates the TC genesis through changes in background lower-level convergence and vorticity, vertical wind shear, and mid-level humidity (Maloney and Hartmann, 2001; Kim et al., 2008; Camargo et al., 2009; Zhao et al., 2015b).

A similar ISO evolution was observed during July and August of both 1996 and 2014. Obvious negative velocity potential anomalies propagated from the Philippines to eastern Pacific from mid-July to mid-August (Figs. 1a-c; Figs. 1f-h). Another region of negative velocity potential anomalies propagated from the South Africa in early August to the Maritime Continent in late August (Figs. 1c-e; Figs. 1h-j). Those two intraseasonal signals are characterized by active and convective phases. Between the two convective phases was an inactive phase characterized by positive velocity potential anomalies that arrived at the Maritime Continent in early August (Fig. 1c and Fig. 1h) and occupied the western Pacific during the whole August (Figs. 1c-e; Figs. 1h-j). Thus, the WNP was dominated by the inactive phases in August of both 1996 and 2014. The intraseasonal anomalies of outgoing long-wave radiation (OLR) averaged in the region of 5°N–15°N, 110°E–160°E from 1979 to 2015 confirmed the two strong ISO inactive phases in August of 1996 and 2014 (Fig. 2c).

According to conventional statistical analysis (Camargo et al. 2009; Cao et al. 2012; Zhao et al. 2015a, b), less TCs should be generated over the WNP in August of these two years. However, extremely different TC genesis numbers were observed. On climatological average, about 5.7 TCs occur in August over the WNP including the South China Sea (Fig. 2a). In August 1996, total 9 TCs formed over the WNP, including three tropical depressions, three tropical storms, one typhoon, one severe typhoon and one super typhoon, which had the second largest number of TCs since 1979 (Fig. 2a). In sharp contrast, there was no TC generated in August 2014 (Fig. 2a). This absence of TC activity in August was observed at the first time since 1945 (Hong et al. 2016).

Previous studies have indicated that the eastward propagating ISO plays an important role in the absence of TCs over the WNP in August 2014 by inducing anomalous easterlies, which led to decreased moisture and vorticity, and increased divergence (Yang et al. 2015; Hong et al. 2016; Bian et al. 2018). The pronounced different TC genesis numbers between 1996 and 2014 suggested that the TC genesis over the WNP in August 1996 must be forced by other factors. This is one issue to be addressed in the present study.

In the traditional method about the impact of the ISO on the TC genesis, the environmental fields in different ISO phases are compared (e.g., Maloney and Hartmann, 2001; Camargo et al. 2009; Zhao et al. 2015a, b). The large-scale factors are in an unfavorable status for the TC genesis during the inactive ISO phase. Cao et al. (2018, 2019a) examined the modulation of the different components of environmental factors on the TC genesis over the WNP from the perspective of the TC genesis time and location. Cao and Wu (2020) contrasted the results of this new perspective with those based on the traditional approach and identified notable differences. The differences are due to a mismatch of the temporal and spatial scales between the intraseasonal background fields and TC genesis. The composite based on local and instantaneous perspective shows that the genesis potential index anomalies are positive in the regions of TC formation, which explain well why there are still TC genesis cases in the inactive ISO phase (Cao and Wu, 2020). Thus, another issue to be addressed in the present study is whether the intraseasonal anomalies of large-scales factors in monthly and daily variations show distinct differences between 1996 and 2014.

The remainder of the paper is arranged as follows. Section 2 describes the data and methods. Section 3 investigates the possible mechanisms that caused the salient differences in TC genesis in August between 1996 and 2014. A summary is provided in Sect. 4.

2. Data And Methods

The TC best-track data over the WNP in the present study were obtained from the Joint Typhoon Warning Center (JTWC), archived in the International Best Track Archive for Climate Stewardship (IBTrACS) v04r00 of the National Climate Data Center (Knapp et al., 2010). This TC track dataset mainly contains the information of TC center, TC date, and the maximum sustained wind speed at the 6-hour intervals. Only

the TCs that the maximum sustained wind speed reaches 25 kts (~12.9 m s^{-1}) over the WNP region from 100°E to 180° and from the equator to 35°N are considered in our analysis.

The daily mean interpolated OLR is obtained from the National Oceanic and Atmosphere Administration (NOAA) satellites (Liebmann and Smith, 1996), which is used as a proxy for deep convection. The monthly mean precipitation is obtained from the Global Precipitation Climatology Project (GPCP) Precipitation data provided by the NOAA/OAR/ESRL PSD, Boulder, Colorado, USA, from their web site at http://www.esrl.noaa.gov/psd/ (Adler et al., 2003). Conventional dynamic and thermodynamic variables come from the ERA5 reanalysis dataset (Hersbach et al., 2020). Those variables from ERA5 have a horizontal resolution of 2.5° × 2.5° in latitude and longitude.

Hsu et al. (2011) showed that there is a palpable peak of spectrum in atmospheric and oceanic variables on the 10–90-day time scale over the WNP. Hong et al. (2016) validated 10–30 days and 30–60 days oscillation in August 2014 by applying wavelet analysis. We derive intraseasonal variations on the 10–90-day band from the original daily time series in 1996 and 2014 by using a 10–90 day Lanczos filter (Duchon, 1979). The synoptic scale variation is on the 3–8-day band extracted by using the same filtering method. The climatological monthly and daily mean based on the time period from 1979 to 2015 is removed from the original data to obtain the monthly and daily anomalies.

In order to exclude the effect of TC circulation on the large-scale flows at 850 hPa, we remove the 850-hPa cyclonic circulations associated with TCs from the original flows before obtaining the variations on the different time scales. The algorithm proposed by Kurihara et al. (1995) is used in the removal of TC-related cyclonic circulation at 850 hPa. The employed procedure is similar as Bi et al. (2015). The outer boundary of TC domain is gained based on the cyclonic circulation at 850 hPa. The details of criterion of the outer boundary and the procedure can be referred in Cao et al. (2019).

3. Factors Responsible For Distinct Tc Genesis In August Of 1996 And 2014

3.1 The wave train

Although intraseasonal velocity potential anomalies at 200 hPa showed the concordant positive anomalies over the whole WNP (Fig. 1), monthly mean wind and OLR anomalies showed a distinct distribution in August of 1996 and 2014. In August 1996, an obvious wave train extended from the South China Sea and southwestern WNP to the middle latitude of the North Pacific (Fig. 3a). Over the South China Sea and southwestern WNP, a strong anticyclonic circulation and inactive convection was located along with the occurrence of four TC cases. In the northeastern WNP, a strong cyclonic circulation and enhanced convection was observed along with the occurrence of five TC cases (Fig. 3a). In contrast, in August 2014, there was no obvious wave train structure of 850-hPa wind anomalies (Fig. 3f). The strong anticyclonic circulation was observed over most of the WNP and a cyclonic circulation was located in the East China Sea (Fig. 3f). This indicates that the anomalous cyclone associated with the wave train was

one of the important factors of the active TC genesis in the northeastern WNP during August 1996. Based on climatological average, only one TC occurs in August in the northeastern WNP. However, total five TCs were generated herein in August 1996, which is the most since 1979 (Fig. 2b). Based on the wind fields with TC signals removed, monthly mean anomalies of 850-hPa winds showed the consistent features in August of 1996 and 2014 (figures not shown).

The averaged OLR anomalies in August 1996 showed active convection around the Maritime Continent and eastern Indian Ocean. From the Maritime Continent to the middle-latitude North Pacific, there was a southwest-northeast -oriented train of negative-positive-negative-positive OLR anomalies, which was consistent with cyclone-anticyclone-cyclone-anticyclone wave train structure of 850-hPa wind anomalies (Fig. 3a). This wave train is associated with the active convection around the Maritime Continent. However, in August 2014, no active convection anomalies were seen over the Maritime Continent, and no corresponding cyclonic circulation was induced over the WNP (Fig. 3f). Positive OLR anomalies and anticyclonic circulation dominated most of the WNP.

The cyclonic circulation created some favorable conditions for the TC genesis in the northeastern WNP. Figures 3b-e showed that there were opposite anomalies of precipitation, mid-level vertical velocity, mid-level specific humidity and lower-level stream function in the northeastern and southwestern WNP in August 1996. In particular, obvious positive precipitation, ascending motion, positive humidity and positive relative vorticity anomalies were located in the northeastern WNP, favorable for the TC genesis herein. In the contrast, negative precipitation, descending motion, weak humidity and negative relative vorticity anomalies occurred over most of the WNP in August 2014, except for limited regions in the East China and Japan (Figs. 3g-j). Those unfavorable conditions resulted in the absence of TC genesis in whole August of 2014.

It is noteworthy that although monthly anomalies of precipitation, vertical motion, specific humidity and relative vorticity were unfavorable, four TCs were still generated in the southwestern WNP during August 1996. It indicates that the TC genesis in the southwestern WNP could not be explained by monthly anomalies of large scale factors. Recent studies have illustrated that the composite based on the local and instantaneous perspective can better reflect the actual environments for the TC genesis (Cao et al., 2018, 2019, Cao and Wu, 2020). Thus, we examine the daily evolution of large-scale conditions to understand the factors responsible for the TC genesis over the WNP in the following section.

3.2 Time evolution of daily anomalies

The four TCs in the southwestern WNP were generated in 4, 12, 16, 21 August of 1996. Figure 4 showed total anomalies (the climatological daily mean removed), intraseasonal anomalies and synoptic anomalies of lower-level winds and relative vorticity at the time of these four TC geneses with the TC signals removed. The total anomalies showed obvious cyclone and positive vorticity around the location of TC genesis on 4 and 21 August of 1996 (Fig. 4a and Fig. 4d). On 12 August of 1996, salient southerly and northerly winds converged along with the positive vorticity anomalies around the location of TC genesis (Fig. 4b). Differently, the TC on 16 August of 1996 was generated in the easterly winds (Fig. 4c). It

indicates that this TC genesis was associated with easterly wave. Previous studies have showed that easterly wave is one of the synoptic-scale perturbations that may induce TC genesis (Fu et al., 2007, Li, 2012). Fu et al. (2007) found that 20% TC geneses during the 2000 and 2001 TC seasons were induced by easterly waves.

A clear southeast-northwest-oriented wave train pattern was observed three days prior to the TC genesis on 16 August 1996 (Fig. 5a). An obvious synoptic-scale cyclone and vorticity anomalies were located around the tropical depression location. On 15 August 1996, the wave train began to weaken (Fig. 5c). On the day of the TC genesis, the synoptic-scale wave train became much weaker (Fig. 5d and Fig. 4k). In the following two days, the synoptic scale wave train started to reinforce (Fig. 5e and Fig. 5f). Particularly, on 18 August 1996, the tropical disturbances had intensified into the tropical storm with the maximum wind of 35 kts (Fig. 5f). It indicates that the intensity of TC experienced two oscillations, which is a common feature during the early stage of TC genesis (Li et al. 2006, Ge et al. 2013, Cao et al. 2016). In the end, the TC gradually intensified into a severe typhoon with the maximum surface wind of 95 kts on 21 August 1996.

Although the monthly mean anomalies of dynamic and thermodynamic variables were favorable for the TC genesis in the northeastern WNP (Fig. 3), it is necessary to investigate the lower-level circulations from the local and instantaneous perspective. As such, Figure 6 showed the total, intraseasonal and synoptic anomalies of lower-level winds and relative vorticity at the time of five TC geneses in the northeastern WNP with the TC signals removed. The common feature of all these five TC cases is that obvious cyclonic circulation and positive relative vorticity occupied the location of TC genesis (Figs. 6a-e). It indicates that both monthly and daily mean anomalies supplied a favorable background for TC genesis in the northeastern WNP.

When the intraseasonal winds and synoptic winds were compared with the total anomalies, it is found that the intraseasonal variation had a larger contribution to TC genesis than synoptic variation in each case on the day of TC genesis (Fig. 4 and Fig. 6). The result of case studies is consistent with the composite analysis in Cao et al. (2018) who showed that the contribution of lower-level vorticity to the TC genesis is mainly due to intraseasonal and synoptic variations with the former slightly larger than the latter.

Based on Fig. 3 and Fig. 4, the daily time evolution of lower-level winds and vorticity showed a completely different distribution from monthly mean anomalies. Although monthly mean anomalies were unfavorable for TC genesis in the southwestern WNP, the daily anomalies at the time of TC genesis provided a favorable environment for the TC genesis. It indicates that monthly mean anomalies of large-scale conditions did not match well the atmospheric states around the location of TC genesis and daily anomalies could reflect well the real background for the TC genesis.

Previous studies about the reasons of the absence of TC genesis in August 2014 were mainly focused on monthly mean anomalies (Hong et al., 2015, Yang et al. 2015). For example, Hong et al. (2015) indicated that the combination of the dry ISO phase and downward motion triggered by the warm sea surface

temperature led to the extremely dry and warm conditions, which were unfavorable for TC genesis over the WNP. However, from the analysis about TC genesis in the southwestern WNP in August 1996, the unfavorable monthly mean anomalies cannot guarantee an inactive TC activity. It is necessary to examine the daily evolution of atmospheric conditions. Figure 7 showed the intraseasonal anomalies of 850-hPa winds and relative vorticity at three-day interval in August 2014. On 4 August 2014, there was an obvious cyclone around 28°N, 148°E (Fig. 7a). However, the cyclonic disturbance was destroyed by the nearby typhoon in the west in the following three days during the western propagation (Fig. 7b). Meantime, another cyclonic disturbance began to develop around the dateline (Fig. 7b). However, the cyclonic disturbance gradually expanded with a larger size and a weaker intensity until disappearance in the following week (Figs. 7d-f). In late August 2014, no obvious potential cyclonic disturbance was observed over the tropical WNP except for easterly winds (Figs. 7g-i). As such, the cyclonic disturbances were suppressed during whole August 2014. It indicates that the suppressed disturbances combined with the inactive ISO phase were responsible for the absence of TC genesis over the WNP in August 2014.

4. Summary

Previous statistical analyses have revealed a tendency for genesis of more and less TCs, respectively, during active and inactive phases of ISO (e.g., Kim et al., 2008; Camargo et al., 2009; Cao and Wu, 2020). An unusual behavior occurred in August 1996 during which nine TC were generated over the WNP, far more than the climatological average of 5.7 TCs. In sharp contrast, no TCs formed over the WNP in August 2014. The present analysis revealed different reasons for the distinct differences of TC genesis in August between 1996 and 2014.

In August 1996, monthly mean anomalies of lower-level wind and convection showed an obvious southwest-northeast-oriented wave train from the Maritime Continent to the mid-latitude central North Pacific associated with the enhanced tropical convection. This wave train resulted in strong anticyclone and suppressed convection in the southwestern WNP and cyclone and enhanced convection in the northeastern WNP, respectively. Correspondingly, dynamical (vorticity and vertical motion) and thermodynamic (precipitation and humidity) conditions are opposite over the northeastern and southwestern WNP. Over the northeastern WNP, the monthly and daily anomalies of large-scale factors provided the favorable background for five TCs in August 1996. In a contrast, over the southwestern WNP, the unfavorable large-scale monthly background cannot explain the genesis of four TCs in August 1996. The daily evolution of atmospheric conditions reveals a common role of the intraseasonal variation of winds and vorticity to these TC geneses, which has a larger contribution than synoptic variation at the time and location of TC genesis.

For the absence of TC genesis in August 2014, in addition to unfavorable monthly anomalies identified in previous studies, the present study reveals the lack of the developing cyclonic disturbances in the daily evolution of wind and vorticity.

Present analysis of two extreme cases of the TC genesis over the WNP suggests that the TC genesis is not only modulated by the ISO phases in a climatological perspective, but also related to local conditions in a short time. This implies that it is necessary to take into consideration the lower-frequency signals in a short time to improve seasonal prediction of the TC genesis.

Declarations

Acknowledgements This study is supported by the 2019 Open Research Program of the Shanghai Typhoon Institute (Grant TFJJ201901), the Open Grants of the State Key Laboratory of Severe Weather (Grant 2020LASW-B01) and the National Natural Science Foundation of China (Grants 41875057 and 41505048).

Data availability statement

The data that support the findings of this study are openly available.

The NOAA OLR data were obtained via https://www.ncdc.noaa.gov/cdr/atmospheric/outgoing-longwave-radiation-daily. The IBTrACS data were obtained from http://www.ncdc.noaa.gov/ibtracs/index.php. The ERA5 data set was obtained from https://cds.climate.copernicus.eu/cdsapp#!/dataset/reanalysis-era5-pressure-levels?tab=form. The GPCP data were obtained via http://www.esrl.noaa.gov/psd/.

References

1. Adler, R.F., G.J. Huffman, A. Chang, R. Ferraro, P. Xie, J. Janowiak, B. Rudolf, U. Schneider, S. Curtis, D. Bolvin, A. Gruber, J. Susskind, and P. Arkin, 2003: The Version 2 Global Precipitation Climatology Project (GPCP) Monthly Precipitation Analysis (1979-Present). *Hydrometeor.*, 4, 1147–1167.
2. Bi, M. Y., **Li, X. Y. Shen**, and M. Peng, 2015: To what extent the presence of real-strength tropical cyclones influences the estimation of atmospheric intraseasonal oscillation intensity? *Atmos. Sci. Let.,* 16, 438–444.
3. Bian, J. P., J. Fang, G. H. Chen, and C. J. Liu, 2018: Circulation features associated with the record-breaking typhoon silence in August 2014. *Atmos. Sci.*, 35(10), 1321–1336.
4. Camargo, S. J., M. C. Wheeler, and A. H. Sobel, 2009: Diagnosis of the MJO modulation of tropical cyclogenesis using an empirical index. *Atmos. Sci.*, 66, 3061–3074.
5. Cao, X., G. H. Chen, T. Li and F. M. Ren, 2016: Simulations of tropical cyclogenesis associated with different monsoon trough patterns over the western North Pacific, *Atmos. Phys.*, 128, 491–511, doi: 10.1007/s00703-015-0428-7.
6. Cao, X., P. Huang, G.-H. Chen, and W. Chen, 2012: Modulation of the western North Pacific tropical cyclone genesis by the intraseasonal oscillation of the ITCZ: A statistical analysis. *Atmos. Sci.*, 29, 744–754.

7. Cao, X., and R. G. Wu, 2020: Comparison of impacts of intraseasonal oscillation on tropical cyclogenesis over the western North Pacific with two methods, *J. Climatol.,* 40(4), 2418–2428.
8. Cao, X., G. Wu, and Mingyu Bi, 2018: Contributions of different time scale variations to tropical cyclogenesis over the western North Pacific. *J. Climate*, 31, 3137–3153, doi: 10.1175/JCLI-D-17-0519.1
9. Cao, X., G. W, M. Y. Bi, X. Q. Lan, Y. F. Dai and J. H. Zhao, 2019: Contributions of different time scale variations to tropical cyclogenesis over the northern tropical Atlantic and comparison with the western North Pacific. *J. Climate*, doi:10.1175/JCLI-D-18-0560.1.
10. Duchan, C. E., 1979: Lanczos filtering in one and two dimensions. *Appl. Meteor.*, 18, 1016–1022.
11. Ge, X. Y., T. Li, M. Peng, 2013: Effects of vertical shears and midlevel dry air on tropical cyclone developments. *Atmos. Sci.,* 70, 3859–3875
12. Fu, B., T. Li, M. S. Peng, , and F. Weng, 2007: Analysis of tropical cyclogenesis in the western North Pacific for 2000 and 2001, *Forecast.*, 22(4), 763-780.
13. Hong, C.-C., M.-Y. Lee, H.-H. Hsu, and T.-C. Chang, 2016: Compounding factors causing the unusual absence of tropical cyclones in the western North Pacific during August 2014, *Geophys. Res. Atmos.*, 121, 9964–9976, doi:10.1002/2016JD025507.
14. Hsu, P.-C., T. Li, and C.-H. Tsou, 2011: Interactions between boreal summer intraseasonal oscillations and synoptic-scale disturbances over the western North Pacific. Part I: energetics diagnosis. *Climate*, 24, 927–941.
15. Huang, P., C. Chou, and R. Huang, 2011: Seasonal modulation of the tropical intraseasonal oscillations on tropical cyclone genesis in the western North Pacific. *Climate*, 24, 6339-6352.
16. Kim, J.-H., C.-H. Ho, H.-S. Kim, C.-H. Sui, and S. K. Park, 2008: Systematic variation of summertime tropical cyclone activity in the western North Pacific in relation to the Madden–Julian oscillation. *Climate*, 21, 1171-1191.
17. Knapp, K. R., M. C. Kruk, D. H. Levinson, H. J. Diamond, and C. J. Neumann, 2010: The International Best Track Archive for Climate Stewardship, IBTrACS. *Amer. Meteor. Soc.,* 91, 363–376.
18. Kurihara, Y., M. A. Bender, R. E. Tuleya, and J. Ross, 1995: Improvements in the GFDL hurricane prediction system. *Mon. Wea. Rev.,* 123, 2791–2801.
19. Li, T., 2012: Synoptic and climatic aspects of tropical cyclogenesis in western North Pacific. Nova Science Publishers, Inc., Eds. K. Oouchi and H. Fudeyasu, Chap.3, 61–94.
20. Li, T., X. Y. Ge, B. Wang, Y. T. Zhu, 2006: Tropical cyclogenesis associated with Rossby wave energy dispersion of a preexisting typhoon. Part II: numerical simulations. *Atmos. Sci.*, 63, 1390–1409.
21. Liebmann, B., H. H. Hendon, and J. D. Glick, 1994: The relationship between tropical cyclones of the western Pacific and Indian Oceans and the Madden-Julian oscillation. *Meteor. Soc. Japan*, 72, 1–412.
22. Liebmann, B., and C. Smith, 1996: Description of a complete (interpolated) outgoing longwave radiation dataset. *Amer. Meteor. Soc.*, 77, 1275–1277.

23. Madden, R., and P. Julian, 1994: Observations of the 40-50-day tropical oscillation-A review. *Wea. Rev.*, 122, 814–837.
24. Maloney, E. D., and D. L. Hartmann, 2001: The Madden-Julian oscillation, barotropic dynamics, and north Pacific tropical cyclone formation. Part I: Observations. *Atmos. Sci.*, 58, 2545–2558.
25. Molinari, J., and D. Vollaro, 2013: What percentage of western North Pacific tropical cyclones form within the monsoon trough? *Wea. Rev.*, 141, 499–505.
26. Ritchie, E. A., and G. J. Holland, 1999: Large-scale patterns associated with tropical cyclogenesis in the western Pacific. *Wea. Rev.*, 127, 2027–2043.
27. Wu, L., Z.-P. Wen, R.-H. Huang, and R. Wu, 2012: Possible linkage between the monsoon trough variability and the tropical cyclone activity over the western North Pacific. *Wea. Rev.*, 140, 140–150.
28. Yang, L., X. Wang, K. Huang, and D. X. Wang, 2015: Anomalous tropical cyclone activity in the Western North Pacific in August 2014. *Amer. Meteor. Soc.*, 96(12), S120-S125.
29. Zhang Q., L. G. Wu, and Q. F. Liu, 2009: Tropical cyclone damages in China 1983-2006. *Amer. Meteor. Soc.*, 90, 489–495.
30. Zhao, C., and T. Li, 2019: Basin dependence of the MJO modulating tropical cyclone genesis. *Climate Dyn.*, 52, 6081–6096.
31. Zhao, H. K., X. Jiang, and L. Wu, 2015a: Modulation of northwest Pacific tropical cyclone genesis by the intraseasonal variability. *Meteor. Soc. Japan*, 93, 81–97.
32. Zhao, H. K., R. Yoshida, and G. B. Raga, 2015b: Impact of the Madden–Julian oscillation on western North Pacific tropical cyclogenesis associated with large-scale patterns. *J. Appl. Meteor. Climatol.*, 54, 1413–1429.

Figures

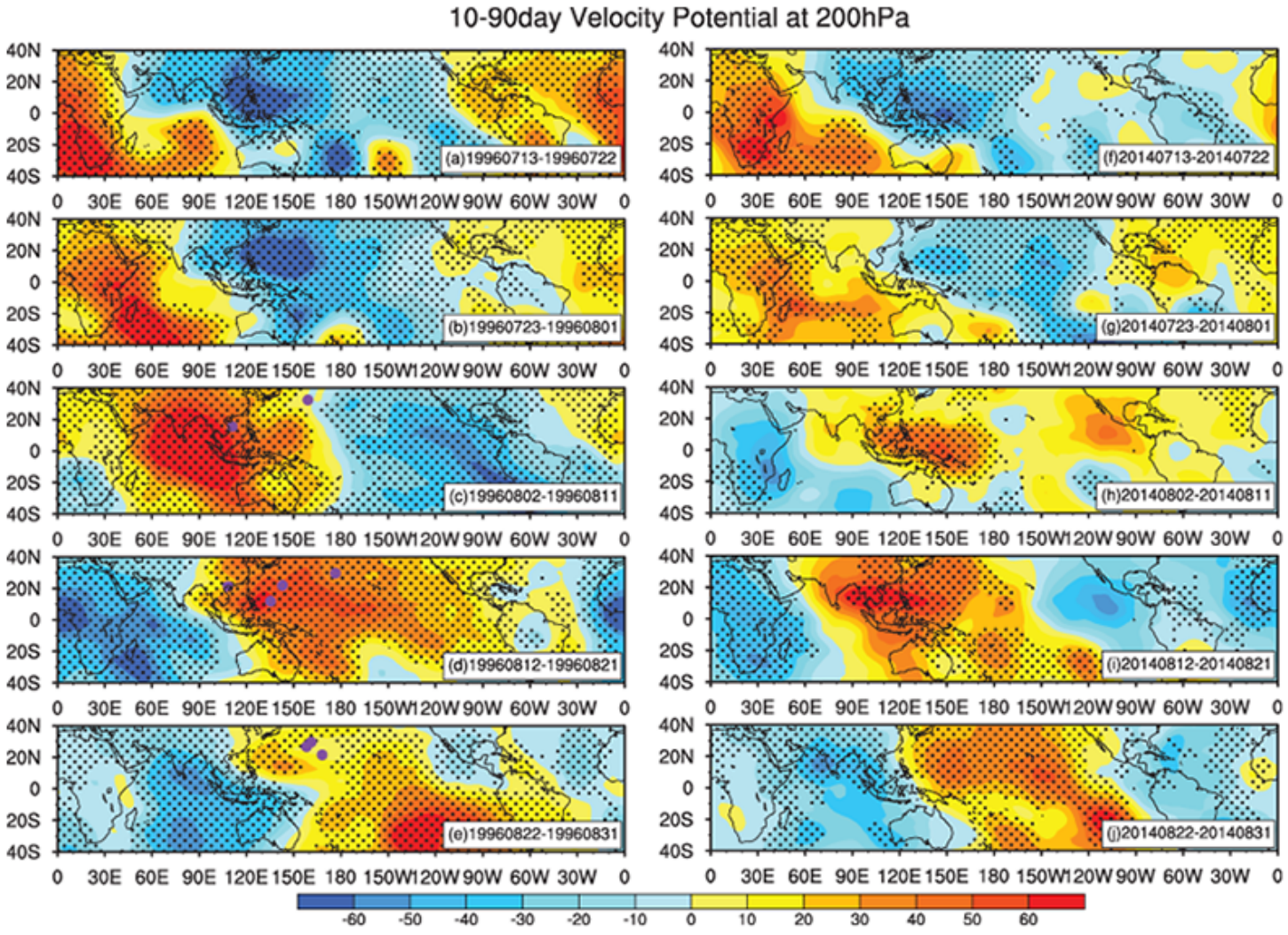

Figure 1

The 10-day averaged 10–90-day filter velocity potential anomalies (105 m2 s-1) at 200 hPa in July and August of (left column) 1996 and (right column) 2014. The black dotted areas denote that the ratio of 10–90-day anomalies to total anomaly was greater than 50%. The purple dots denote the TC genesis location. Note: The designations employed and the presentation of the material on this map do not imply the expression of any opinion whatsoever on the part of Research Square concerning the legal status of any country, territory, city or area or of its authorities, or concerning the delimitation of its frontiers or boundaries. This map has been provided by the authors.

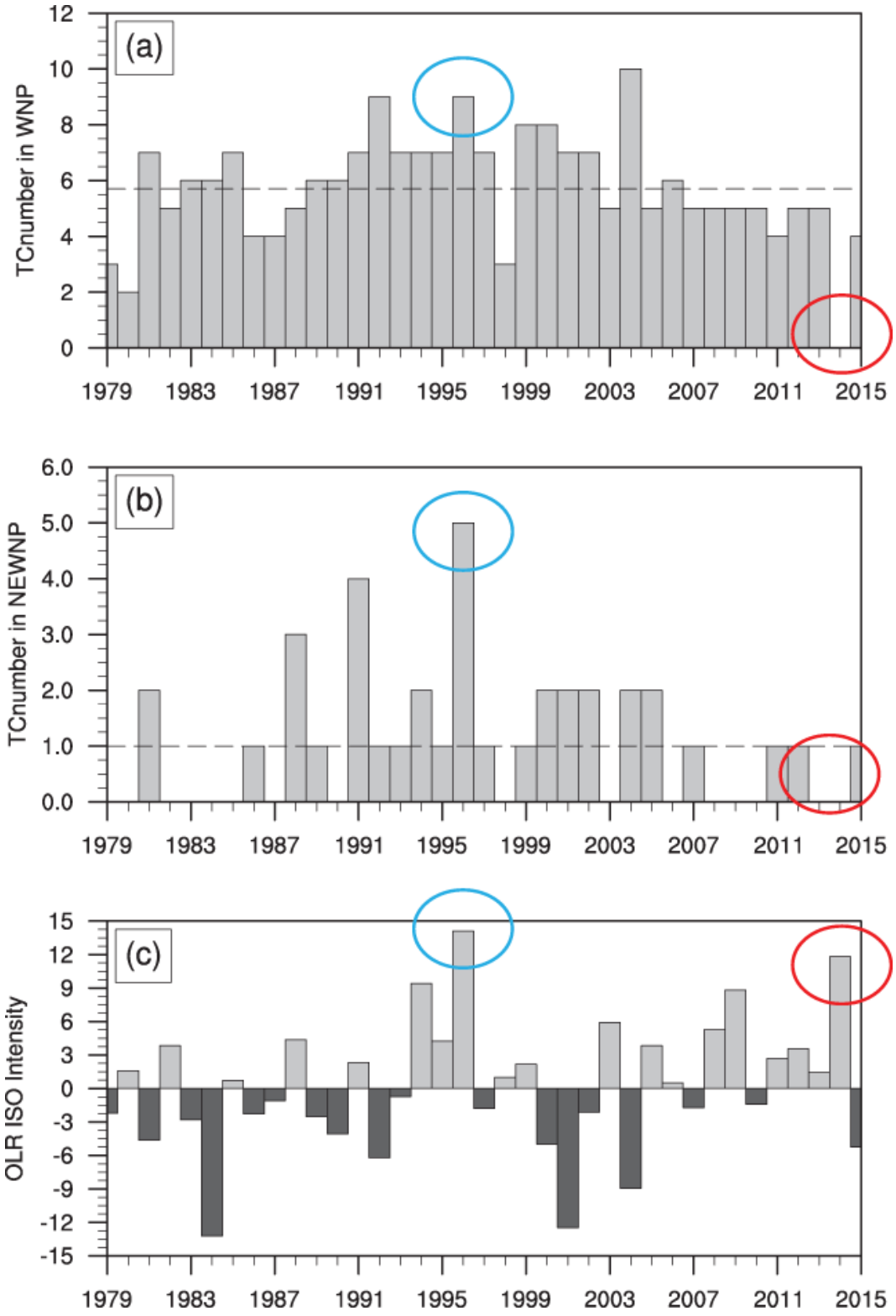

Figure 2

The TC genesis number (a) in the whole WNP and (b) in the region of 15°–35°N, 150°–180°E, and (c) the interannual variation of intraseasonal OLR averaged in the region of 5–15°N, 110–160°E in August from 1979 to 2015. The cyan circle denotes the year of 1996 and the red circle denotes the year of 2014.

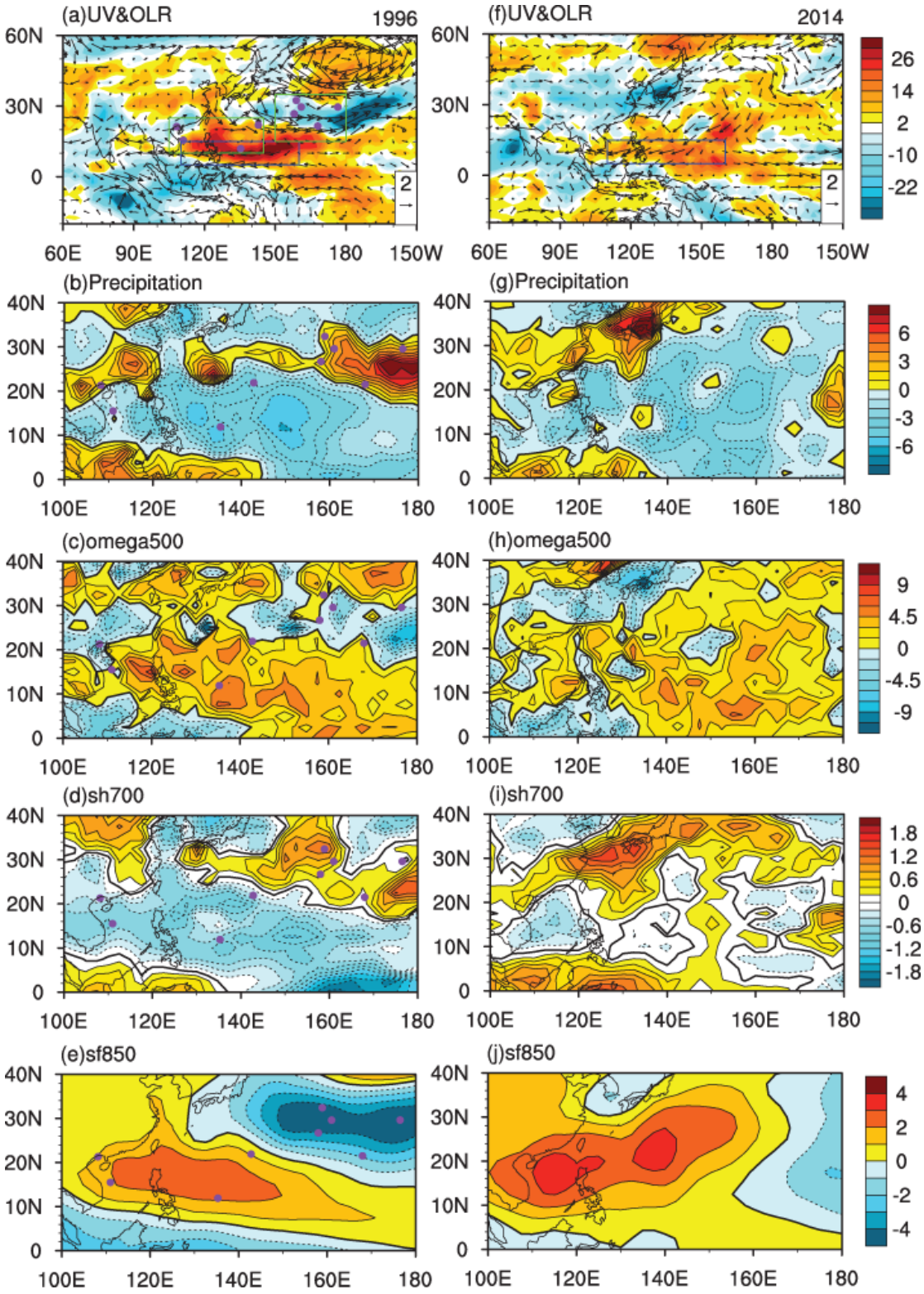

Figure 3

Monthly mean anomalies of (a, f) 850 hPa wind (m s-1) and OLR (W m2), (b, g) precipitation (mm day-1), (c, h) vertical velocity (10-2 Pa s-1) at 500 hPa, (d, i) specific humidity (g kg-1) at 700 hPa, and (e, j) stream function (106 m2 s-1) at 850 hPa in August of (left column) 1996 and (right column) 2014. The blue rectangles in (a) and (b) denote the region which is used to calculate the ISO. The green rectangles in (a) denote the two major TC genesis regions. The purple dots denote the TC genesis location. Note: The

designations employed and the presentation of the material on this map do not imply the expression of any opinion whatsoever on the part of Research Square concerning the legal status of any country, territory, city or area or of its authorities, or concerning the delimitation of its frontiers or boundaries. This map has been provided by the authors.

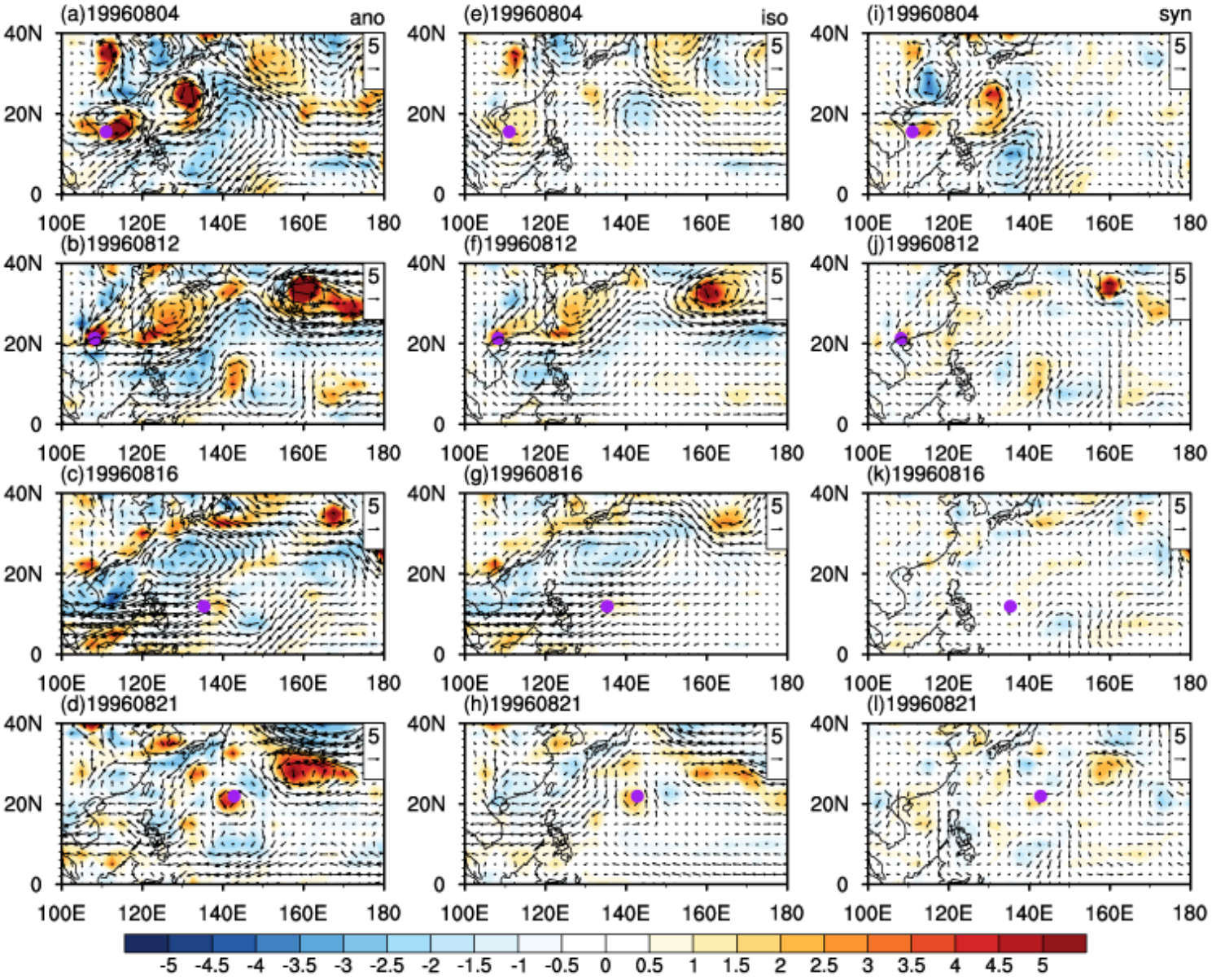

Figure 4

The daily (a-d) total anomalies, (e-h) intraseasonal anomalies and (i-l) synoptic anomalies of 850-hPa winds (m s-1) and relative vorticity (10-5 s-1) on August 4 (the first row), 12 (the second row), 16 (the third

row) and 21 (the fourth row) of 1996 with the TC signals removed. The purple dots denote the TC genesis location.

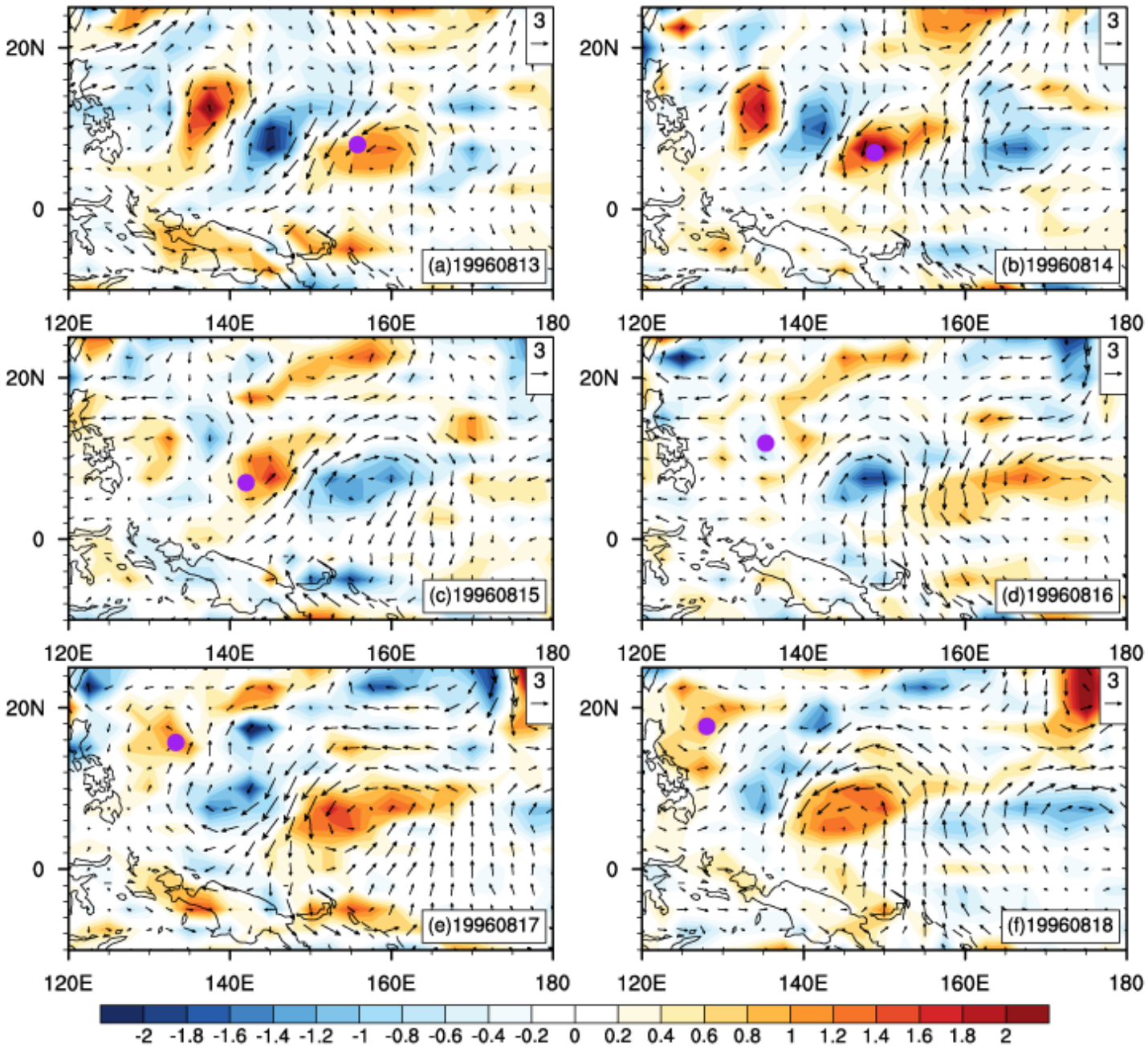

Figure 5

The synoptic anomalies of 850-hPa winds (m s-1) and relative vorticity (10-5 s-1) from 13 August to 18 August 1996 at one day interval with the TC signals removed. The purple dots denote the location of TC.

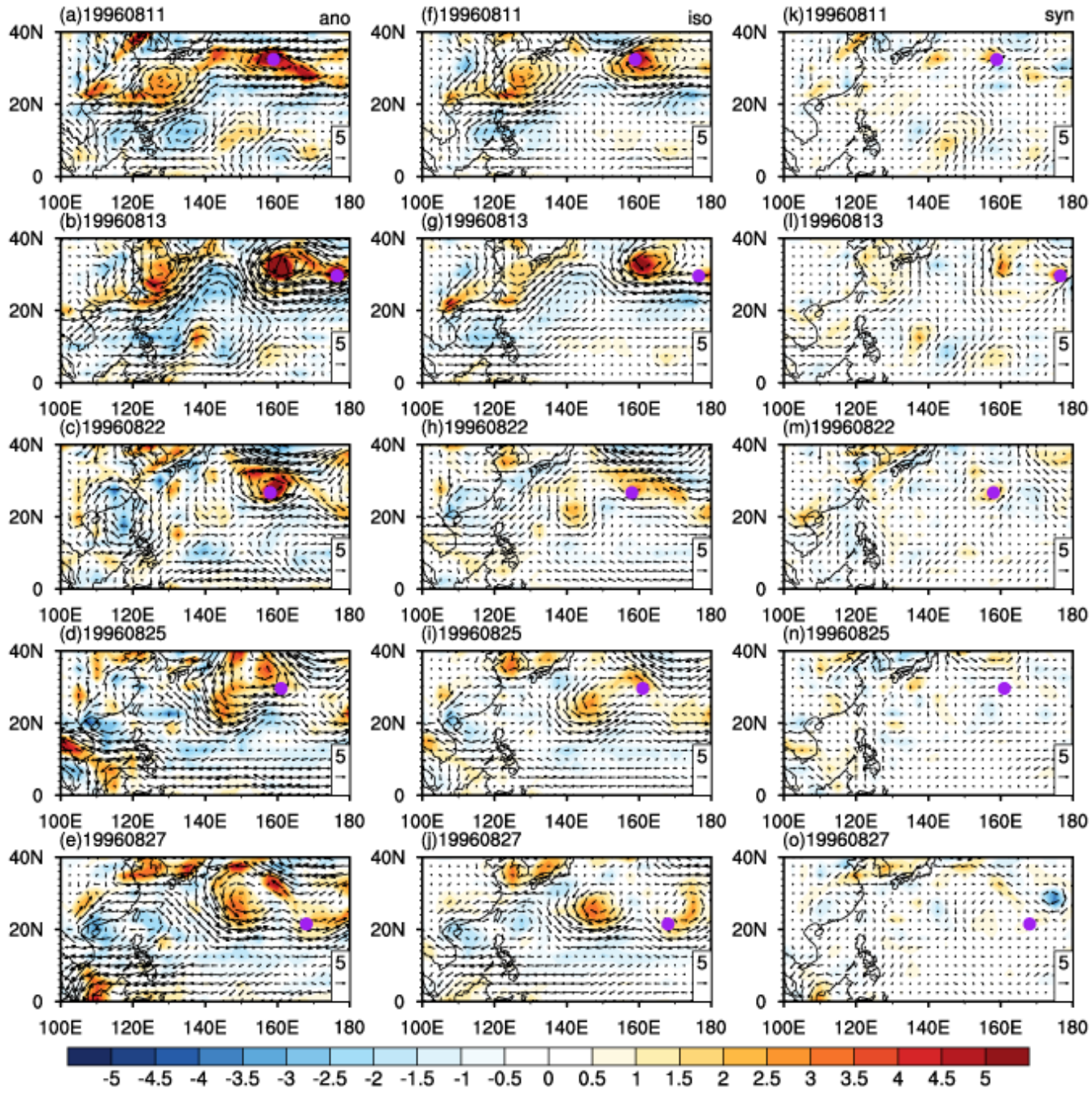

Figure 6

The daily (a-e) total anomalies, (f-j) intraseasonal anomalies and (k-o) synoptic anomalies of 850-hPa winds (m s-1) and relative vorticity (10-5 s-1) on August 11 (the first row), 13 (the second row), 22 (the third row), 25 (the fourth row) and 27 (the fifth row) of 1996 with the TC signals removed. The purple dots denote the TC genesis location.

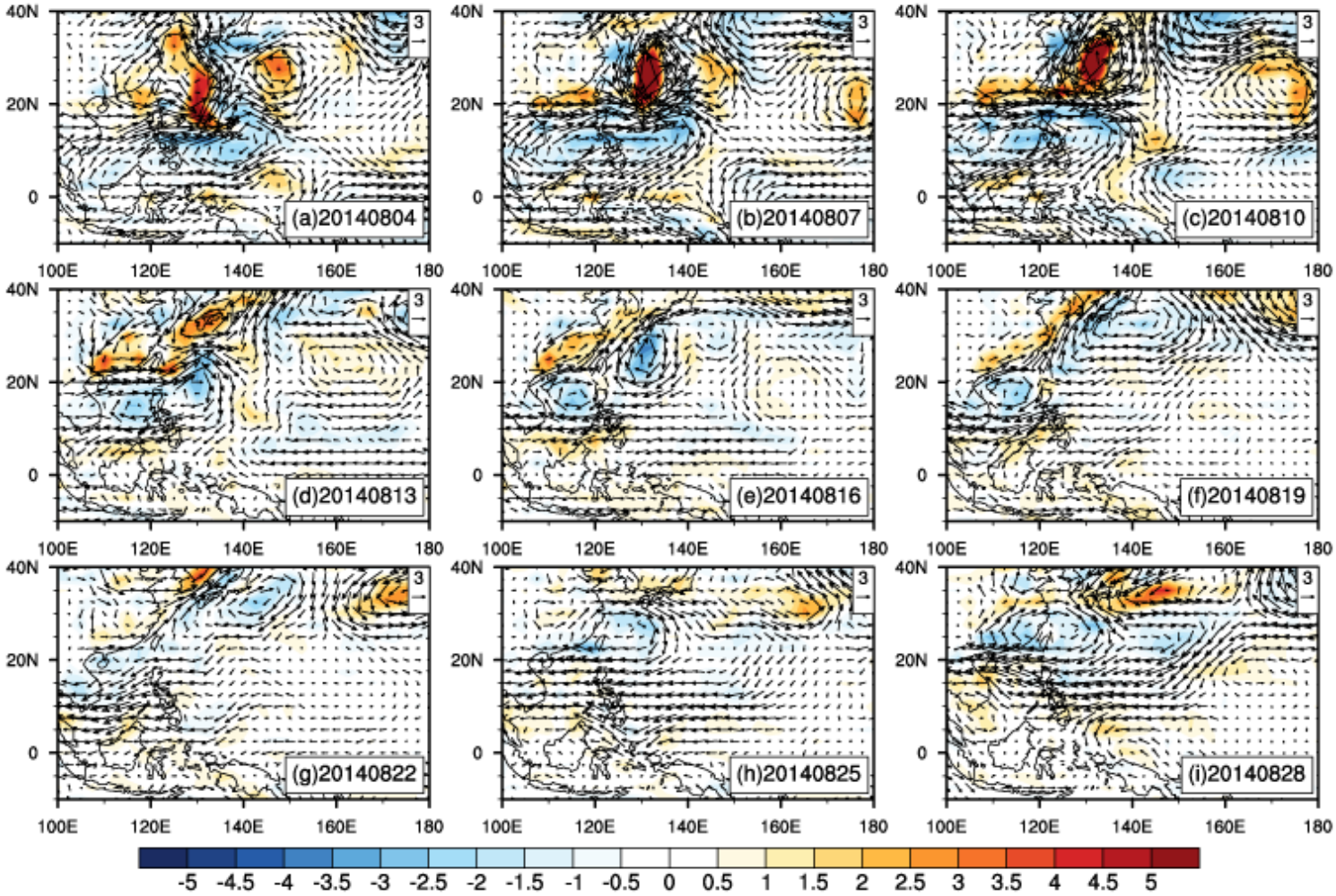

Figure 7

The intraseasonal anomalies of 850-hPa winds (m s-1) and relative vorticity (10-5 s-1) at three day interval of August 2014.